Nanotechnology 19 (2008) 455301 (4pp) doi:10.1088/0957-4484/19/45/455301

# Fabrication of sub-25 nm diameter pillar nanoimprint molds with smooth sidewalls using self-perfection by liquefaction and reactive ion etching

**Qiangfei Xia and Stephen Y Chou**[1]

NanoStructure Laboratory, Department of Electrical Engineering, Princeton University, Princeton, NJ 08544, USA

E-mail: chou@princeton.edu

Received 20 July 2008, in final form 2 September 2008
Published 8 October 2008
Online at stacks.iop.org/Nano/19/455301

**Abstract**
Self-perfection by liquefaction (SPEL) was used to fabricate nanoimprint molds with an array of sub-25 nm diameter pillars (200 nm period), resulting in nearly perfect cylindrical shape and smooth sidewalls. SPEL turned an array of irregularly shaped Cr polygons into an array of nearly perfect circular dots with small diameter. The Cr dot arrays were then transferred to $SiO_2$ or Si pillar arrays by means of reactive ion etching to produce imprint molds. High-fidelity nanoimprint lithography using the pillar molds was also demonstrated.

(Some figures in this article are in colour only in the electronic version)

Nanoimprint lithography (NIL) is a low-cost, high-throughput patterning technique with demonstrated sub-3 nm pattern duplication capabilities [1–3]. One of the key requirements for successful NIL is a high-quality mold. However, as feature sizes approach 10 nm and below, the noise in conventional mold fabrication processes such as electron beam lithography (EBL) may significantly deform the intended shape and cause significant edge roughness. Other mold fabrication methods such as interference lithography [4], proton beam writing [5], focused ion beam writing [6], and x-ray lithography [7] encounter similar noise problems, since they all utilize particle beams which intrinsically have fluctuations in their energy and momentum.

To overcome this problem, this paper applies self-perfection by liquefaction (SPEL) to improve fabrication of nanoimprint molds. SPEL repairs defects and/or enhances nanostructure shapes after their initial fabrication by selectively melting nanostructures for a short period of time (hundreds of nanoseconds) during which the surface tension smoothes out the defects [8–10]. Using SPEL and reactive ion etching (RIE), we have made smooth cylindrical Si and $SiO_2$ pillars as small as 25 nm diameter over a large area for imprint molds.

The principle of our mold fabrication method is illustrated in figure 1. First, nanoscale metal pads (Cr in this study) are fabricated on a substrate. The Cr pads usually have increasingly severe rough edges as they become smaller due to the intrinsic noise in their fabrication methods (figure 1(a)). Next, SPEL is used, where a laser pulse selectively melts the Cr pads, and the surface tension reforms these pads into round droplets (figures 1(b), (c)). The round shape of these droplets is preserved after the metal resolidification (figure 1(d)). These round Cr dots are then used as masks for RIE of the material underneath (figure 1(e)). After stripping off the Cr masks, cylindrical pillars with smooth sidewalls remain on the substrate (figure 1(f)).

Different from isothermal heating of EBL patterned metal nanodots [11], SPEL uses a single laser pulse to cause a thorough melting the metal patterns on a substrate in less 1 ns without significantly heating of the substrate, resulting in ultrafast and local heating, better metal shapes, and thus well suited for a wide range of applications. In comparison with the method of isothermal heating, pulsed excimer laser heating has two advantages: (a) it allows selectively and locally surface melting of a high temperature material without damage

[1] Author to whom any correspondence should be addressed.

 © 2008 IOP Publishing Ltd Printed in the UK

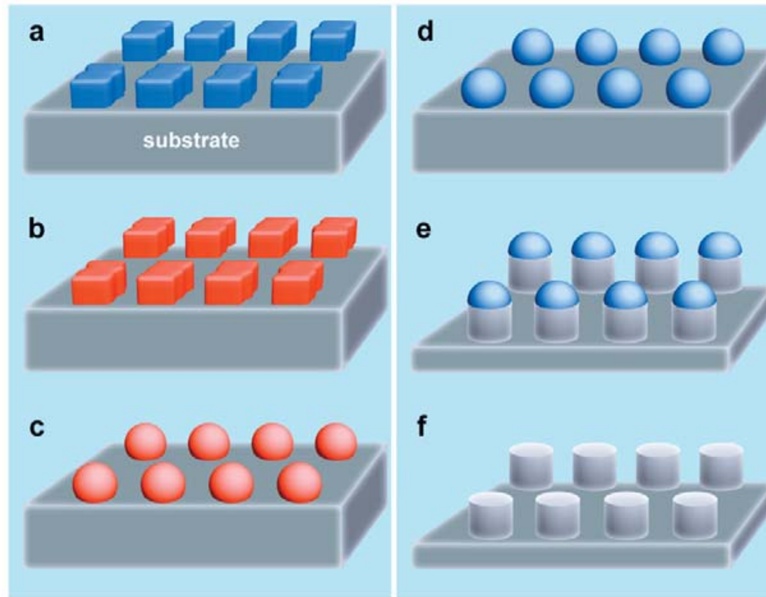


**Figure 1.** Schematic of our process to make cylindrical pillar molds. (a) Metal nanostructures with geometrical defects. (b) The nanostructures in (a) are melted. (c) The molten material reflows into round dots to minimize the surface energy. (d) After resolidification, the rough-edged pads turn into smooth round dots. (e) These round metal dots are used as a hard etching mask for RIE. (f) The metal mask is stripped off before the pillar mold is ready for use.

the substrate; and (b) it can achieve single dot per original pad (due to a higher metal atom mobility at a higher temperature).

In fabrication of the Cr pads, a thin layer of thermoplastic resist (NXR-1020, Nanonex Corp., Monmouth Junction, NJ) was first spin-coated on a fused silica (FS) or Si substrate. After baking on a hot plate to drive out the residual solvent, the resist was patterned by thermal NIL (Nanonex NX-2000) with a pillar mold, followed by $O_2$ RIE of the residual resist layer. To illustrate the effectiveness of SPEL, a pillar mold with poor pillar shape was used intentionally. A thin layer of Cr was deposited on the substrates by an electron beam evaporator and arrays of Cr pads were made on the substrates after a lift-off process. In SPEL experiments, a single laser pulse ($\lambda = 308$ nm, pulse width 20 ns, spot size 3 mm by 3 mm) was used to expose the rough-edged Cr pad array, resulting in near-perfect circular dots. The Cr pads selectively absorb the laser pulse while the FS substrate is transparent to the laser pulse.

In pattern transfer, these circular Cr dot arrays were used as etching mask of RIE of $SiO_2$ or Si (Plasma Therm 2486, Plasmatherm, St. Petersburg, FL). A low base pressure was used in RIE for a low etching rate ($\sim$3 nm min$^{-1}$) and hence smooth sidewalls. After RIE, the Cr mask on top was stripped off using Cr etchant CR-7 (Cyantek Corp, Fremont, CA).

We found that in SEPL a single laser pulse was sufficient to melt each of the rough-edged Cr pads into one near-perfect circular dot. For example, using a pulse of 420 mJ cm$^{-2}$, Cr pads of 20 nm thick and 140 nm by 110 nm in size on fused silica (FS) become nearly perfect circular dots of 80 nm diameter (figures 2(a), (b)). Atomic force microscope (AFM) measurements showed that the height of these dots was about 48 nm. These round Cr dots were then used as a mask during RIE of the FS to get cylindrical pillars with a height of 200 nm (figure 2(d)), and smooth side walls (figure 2(f)). For a direct comparison with the pillars fabricated using the unsmoothed Cr pads as etching mask (figures 2(c) and (e)), the edge roughness from the original Cr pad mask was transferred to the pillars. The mold fabrication certainly can be extended to other substrates such as Si.

To further check the quality of the nearly perfect pillar molds fabricated by SEPL, we used them to imprint resists. Before the imprinting, the new molds were cleaned by RCA and treated with an anti-adhesion layer. Both UV and thermal nanoimprints were successful (the resists were NXR-1020 for thermal NIL and NXR-3020 for UV-NIL, respectively). For instance, with a 25 nm diameter Si pillar mold fabricated using SPEL and RIE, 25 nm diameter holes were imprinted into a NXR-1020 resist film on a Si substrate with high fidelity (figure 3). A close examination of the holes revealed that the holes had round shape and uniform size distribution, indicating high-quality mold and high-fidelity pattern transfer.

Furthermore, we have extended this method to fabricate large-area NIL molds (as large as 1 inch by 1 inch) by a step and repeat exposure scheme, with a 200 $\mu$m stitching area between each laser spot (figure 4(a)). Although the overlapping areas between different laser pulses have been exposed 2 or 4 times, the diameter of the resultant circular Cr dots is nearly the same as those with a single pulse (figures 4(b), (c)). This is expected since the final dot diameter should be dependent on the total material volume and the contact angel as discussed below.

Another important advantage of open-SPEL is that it not only makes the shape nearly perfect round, but also reduces the original size. The final dot diameter after SPEL can be

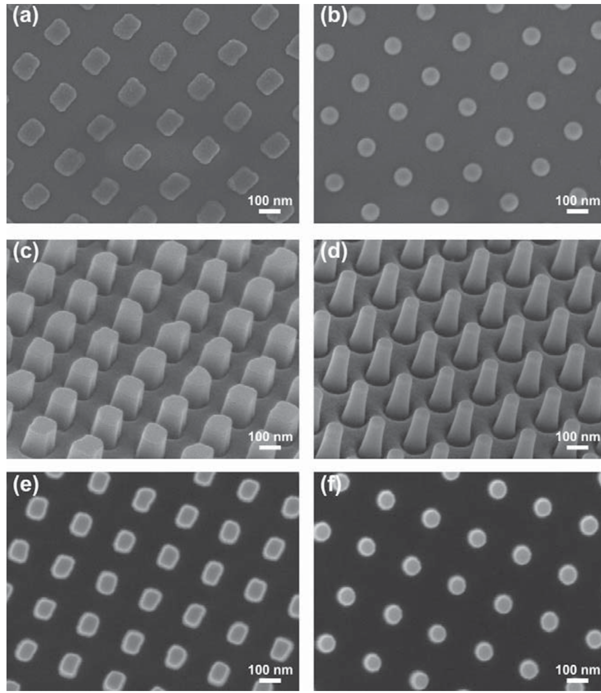


**Figure 2.** (a) Cr squares of 140 nm by 110 nm and 20 nm thickness on a fused silica substrate made by NIL. (b) After SPEL, the irregular squares in (a) became nearly perfect round dots of 80 nm diameter and 48 nm height. (c) Rough pillars etched into FS using Cr pads in (a) as an etching mask. (d) Smooth round pillars etched into FS using round Cr dots in (b) as an etching mask. (e) and (f) are top view images of pillars in (c) and (d), respectively, which show the etching fidelity during RIE.

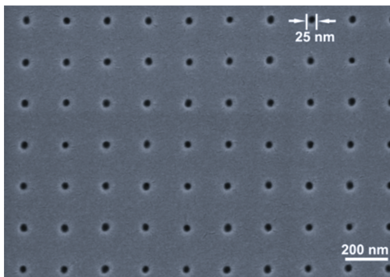


**Figure 3.** 25 nm diameter hole array in thermal plastic resist (NXR-1020) imprinted using a Si pillar mold that was fabricated by SPEL and RIE.

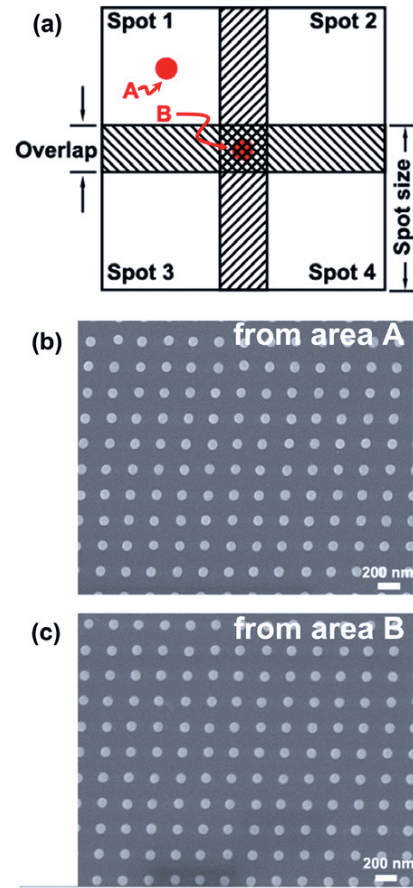


**Figure 4.** (a) Schematic of step and repeat exposure with a 200 $\mu$m overlap (shadowed area) in SPEL; (b) and (c) are SEM images from spot A and B in (a), which shows that multiple exposure in the overlapped area during SPEL results in the same high-quality round metal dots on FS.

estimated from the constant material volume $V$ and contact angle $\theta$ (figures 5(a), (b)). If we assume the dot is a segment of a perfect sphere, its volume is:

$$V = \frac{\pi h}{6}(3r^2 + h^2) = \frac{\pi R^3}{3}(2 - 3\cos\theta + \cos^3\theta),$$

where $h$ is the height of the cap, $r$ the diameter of the cap, $R$ the diameter of the hosting sphere, and $\theta$ the contact angle.

Because the $h$ of partial sphere is often many times larger than the initial pattern thickness, the diameter of the final partial sphere formed by melting the pattern will be smaller than the lateral dimension of the initial pattern. The diameter, $d$, of the pillar etched using the partial sphere as the etching mask is given by:

$$d = \begin{cases} 2r = 2\left[\dfrac{3V}{\pi(2 - 3\cos\theta + \cos^3\theta)}\right]^{\frac{1}{3}} \sin\theta, \\ \qquad \text{for } \theta < 90^\circ \\ 2R = 2\left[\dfrac{3V}{\pi(2 - 3\cos\theta + \cos^3\theta)}\right]^{\frac{1}{3}}, \\ \qquad \text{for } \theta \geqslant 90^\circ. \end{cases}$$

The dependence of the effective metal dot diameter on the volume of the metal for materials with different contact angles (we use 60° and 140° in the calculation) was plotted in figure 5(c). Clearly, with less material and/or a larger contact angle, the dot size becomes smaller. This suggests that our method is capable of making sub-10 nm circular dots and sub-10 nm cylindrical imprint molds.

Based on the principle and experimental results, we have demonstrated that SPEL has several advantages in making small feature size pillar imprint molds with fewer defects. In

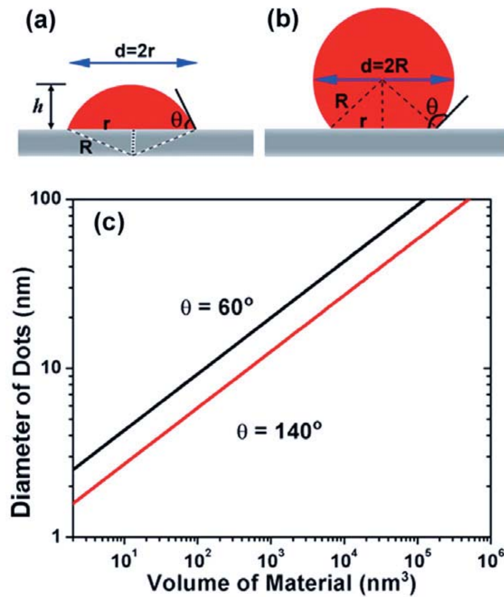


**Figure 5.** Schematic of effective metal dot diameter when the contact angle between the dot and the substrate is (a) smaller than 90° and (b) larger than or equal to 90°. (c) Calculated dependence of metal dot diameter on the material volume for the materials with contact angles (to the substrate) of 60° and 140°, respectively.

addition to a nearly perfect round shape, a small feature size structure can be made from an initially larger one. SPEL can improve the size uniformity of the metal dots while maintaining the original periodicity. SPEL is not limited by the substrate as is the case for EBL, where very small structures are difficult to fabricate on non-conductive substrates. Using SPEL with step and repeat exposure, larger area mold with near-perfect cylindrical pattern can be made with high throughput.

In summary, we have used SPEL to make nanoimprint molds with arrays of cylindrical pillars having smooth sidewalls and sub-25 nm feature size. The molds were used for nanoimprinting successfully. The size of the final structure can be tuned by tailoring the amount of material deposited, and the interfacial properties between the metal and the substrate. This method works for different substrates with high throughput and low cost, and it can shrink the feature size into sub-10 nm regime.

## Acknowledgments

This work is supported partially by the Defense Advanced Research Projects Agency (DARPA) and the Office of Naval Research (ONR). Q Xia thanks D Zhang for help in the schematic illustrations and K J Morton for some original molds.

## References

[1] Chou S Y, Krauss P R and Renstrom P J 1995 *Appl. Phys. Lett.* **67** 3114–6
[2] Chou S Y, Krauss P R and Renstrom P J 1996 *Science* **272** 85–7
[3] Austin M D, Ge H X, Wu W, Li M T, Yu Z N, Wasserman D, Lyon S A and Chou S Y 2004 *Appl. Phys. Lett.* **84** 5299–31
[4] Park S, Schift H, Solak H H and Gobrecht J 2004 *J. Vac. Sci. Technol.* B **22** 3246–50
[5] Ansari K, van Kan J A, Bettiol A A and Watt F 2004 *Appl. Phys. Lett.* **85** 476–8
[6] Watanabe K *et al* 2004 *J. Vac. Sci. Technol.* B **22** 22–6
[7] Junarsa I and Nealey P F 2004 *J. Vac. Sci. Technol.* B **22** 2685–90
[8] Chou S Y and Xia Q F 2005 *EIPBN'05: The 49th Int. Conf. on Electron, Ion and Photon Beam Technology and Nanofabrication (Grande Lakes, Orlando, FL, May–June 2005)*
[9] Xia Q F and Chou S Y 2005 *NNT'05: The 4th Int. Conf. on Nanoimprint and Nanoprint Technology (Nara, Oct. 2005)*
[10] Chou S Y and Xia Q F 2008 *Nat. Nanotechnol.* **3** 295–300
[11] Javey A and Dai H J 2005 *J. Am. Chem. Soc.* **127** 11942–3